

Advanced Healthcare Materials

Liquefied microcapsules as dual-microcarriers for 3D+3D bottom-up tissue engineering --Manuscript Draft--

Manuscript Number:	adhm.201901221R1
Full Title:	Liquefied microcapsules as dual-microcarriers for 3D+3D bottom-up tissue engineering
Article Type:	Full Paper
Section/Category:	
Keywords:	Cell encapsulation, bottom-up tissue engineering, microparticles, osteogenic differentiation, co-culture
Corresponding Author:	Clara R Correia, MSc, PhD Universidade de Aveiro CICECO Aveiro, Aveiro PORTUGAL
Additional Information:	
Question	Response
Please submit a plain text version of your cover letter here.	<p>Dear editor,</p> <p>We present the manuscript entitled “Liquefied microcapsules as dual-microcarriers for 3D+3D bottom-up tissue engineering” that we would like you to consider for resubmission in Advanced Healthcare Materials (adhm.201900795, editor: Dr. Uta Goebel). We performed all the minor corrections detected by the reviewer, as specified in the “point-by-point response” document. Additionally, we performed two minor corrections in the figures:</p> <ul style="list-style-type: none"> - Figure 3E: the weight of the arrow was increased for enhance the visualization of the object; - Figure S1: a new block showing the top-view visualization of the capsules was added to clarify design of the experiment. <p>We are fully available to provide any further information you may need.</p> <p>Sincerely, Clara R. Correia (Junior Researcher) and João F. Mano (Full Professor) CICECO-Aveiro Institute of Materials, Dept. Chemistry, University of Aveiro, Aveiro, Portugal</p>
Do you or any of your co-authors have a conflict of interest to declare?	No. The authors declare no conflict of interest.
Corresponding Author Secondary Information:	
Corresponding Author's Institution:	Universidade de Aveiro CICECO
Corresponding Author's Secondary Institution:	
First Author:	Clara R Correia, MSc, PhD
First Author Secondary Information:	
Order of Authors:	Clara R Correia, MSc, PhD
	Isabel M. Bjørge, MSc
	Jinfeng Zeng

	Michiya Matsusaki
	João F. Mano, BSc, MSc, PhD, Full Professor
Order of Authors Secondary Information:	
Abstract:	<p>Cell encapsulation systems must ensure the diffusion of molecules to avoid the formation of necrotic cores. The architectural design of hydrogels, the gold standard tissue engineering strategy, is thus limited to a microsize range. To overcome such limitation, liquefied microcapsules encapsulating cells and microparticles are proposed. Microcapsules with controlled average diameters of $608.5 \pm 122.3 \mu\text{m}$ are produced at high rates by electrohydrodynamic atomization, and RGD domains are introduced in the multilayered membrane. While cells and microparticles interact towards the production of confined microaggregates, on the outside cell-mediated macroaggregates are formed due to the aggregation of microcapsules. The concept of simultaneous aggregation is herein termed as 3D+3D bottom-up tissue engineering. Microcapsules are cultured alone (microcapsule1) or on top of 2D cell beds composed of HUVECs alone (microcapsule2) or co-cultured with fibroblasts (microcapsule3). Microcapsules are able to support cell encapsulation shown by LiveDead, MTS and dsDNA assays. Only microcapsule 3 are able to form macroaggregates, as shown by F-actin immunofluorescence. The bioactive 3D system also presented alkaline phosphatase activity, thus allowing osteogenic differentiation. Upon implantation using the chick chorioallantoic membrane (CAM) model, microcapsules recruit a similar number of vessels with alike geometric parameters in comparison with CAMs supplemented with bFGF.</p>

Dear editor,

We present the manuscript entitled “*Liquefied microcapsules as dual-microcarriers for 3D+3D bottom-up tissue engineering*” that we would like you to consider for resubmission in *Advanced Healthcare Materials* (adhm.201900795, editor: Dr. Uta Goebel). We performed all the minor corrections detected by the reviewer, as specified in the “point-by-point response” document. Additionally, we performed two minor corrections in the figures:

- Figure 3E: the weight of the arrow was increased for enhance the visualization of the object;
- Figure S1: a new block showing the top-view visualization of the capsules was added to clarify design of the experiment.

We are fully available to provide any further information you may need.

Sincerely,

Clara R. Correia (Junior Researcher) and João F. Mano (Full Professor)

CICECO-Aveiro Institute of Materials, Dept. Chemistry, University of Aveiro, Aveiro,
Portugal

Liquefied microcapsules as dual-microcarriers for 3D+3D bottom-up tissue engineering

Clara R. Correia^{a}, Isabel M. Bjørge^a, Jinfeng Zeng^b, Michiya Matsusaki^{b,c,d}, João F. Mano^{a*}*

Dr. C.R. Correia*, I.M. Bjørge, and Professor J.F. Mano*

CICECO-Aveiro Institute of Materials, Department of Chemistry, Campus Universitário de Santiago, 3018-193 Aveiro, Portugal

E-mails: claracorreia@ua.pt and jmano@ua.pt

Dr. J. Zeng

Osaka University, Joint Research Laboratory (TOPPAN) for Advanced Cell Regulatory Chemistry, Graduate School of Engineering, Japan

Professor M. Matsusaki

Osaka University, Joint Research Laboratory (TOPPAN) for Advanced Cell Regulatory Chemistry, Graduate School of Engineering, Japan

Division of Applied Chemistry, Graduate School of Engineering, Osaka University, Japan

JST, PRESTO, Japan

Keywords: microcapsules, cell encapsulation, layer-by-layer, bottom-up tissue engineering, 3D systems

Abstract

Cell encapsulation systems must ensure the diffusion of molecules to avoid the formation of necrotic cores. The architectural design of hydrogels, the gold standard tissue engineering strategy, is thus limited to a microsize range. To overcome such limitation, liquefied microcapsules encapsulating cells and microparticles are proposed. Microcapsules with

1 controlled sizes with average diameter of $608.5 \pm 122.3 \mu\text{m}$ are produced at high rates by
2 electrohydrodynamic atomization, and RGD domains are introduced in the multilayered
3 membrane. While cells and microparticles interact towards the production of confined
4 microaggregates, on the outside cell-mediated macroaggregates are formed due to the
5 aggregation of microcapsules. The concept of simultaneous aggregation is herein termed as
6
7 3D+3D bottom-up tissue engineering. Microcapsules are cultured alone (microcapsule¹) or on
8 top of 2D cell beds composed of HUVECs alone (microcapsule²) or co-cultured with fibroblasts
9 (microcapsule³). Microcapsules are able to support cell encapsulation shown by LiveDead,
10 MTS and dsDNA assays. Only microcapsule³ are able to form macroaggregates, as shown by
11 F-actin immunofluorescence. The bioactive 3D system also presented alkaline phosphatase
12 activity, thus allowing osteogenic differentiation. Upon implantation using the chick
13 chorioallantoic membrane (CAM) model, microcapsules recruit a similar number of vessels
14 with alike geometric parameters in comparison with CAMs supplemented with bFGF.
15
16
17
18
19
20
21
22
23
24
25
26
27
28
29
30

31 **1. Introduction**

32 Liquefied cell culture systems have emerged as an alternative to solve some specific drawbacks
33 presented by the classical 3D tissue engineering strategies, namely the encapsulation of cells
34 within hydrogels.^[1] The main advantages of hydrogels as cell encapsulation matrixes are their
35 hydrophilic nature, and their ability to provide a three-dimensional (3D) environment. However,
36 key parameters when designing hydrogels include architectural factors, such as size and porous
37 structure, which are limited to a specific range due to mass transportation concerns.^[2] If cells
38 encapsulated at the core are deprived from a proper diffusion of essential molecules, they will
39 inevitably undergo apoptosis. Liquefying the core of hydrogels seemed a logical and simple
40 approach, however, long-term application of such systems failed because all normal tissue-
41 derived cells, excepting hematopoietic progenitor cells, are anchorage-dependent. When
42 deprived from a physical support, these cells are not able to proliferate, and consequently
43
44
45
46
47
48
49
50
51
52
53
54
55
56
57
58
59
60
61
62
63
64
65

1 undergo anoikis.^[3] In the last years, we have been successfully exploring an alternative
2 approach that combines the advantages of hydrogels, liquefied systems, and microcarriers.
3
4 Besides solving the limited diffusion of hydrogels, liquefied capsules also allow the
5 encapsulated cells to self-organize within the liquefied core, rather than pre-establishing their
6
7 3D organization. Additionally, liquefied capsules can be implanted by injection, thus allowing
8
9 minimal invasive procedures, even when presenting macrosized diameters^[4]. We established the
10
11 concept of liquefied and multilayered capsules, with promising results *in vitro* and *in vivo* for
12
13 general or more applied tissue engineering strategies for cartilage and bone regeneration.^[4-8]
14
15 The concept relies on the use of alginate hydrogels as temporary hydrophilic 3D structure to
16
17 encapsulate cells and microparticles. After the build-up of a multilayered membrane, the core
18
19 can be subsequently liquefied by a simple mild process. The nanostructure of this membrane
20
21 assures the rapid exchange of biomolecules essential for long-term cell survival and signaling.
22
23 The encapsulated microparticles act as cell microcarriers by providing the physical support
24
25 required for cells to survive. Within the liquefied core, cells can move freely, interact directly
26
27 with other co-encapsulated cells, and, most importantly, create cell-mediated aggregates by
28
29 recruiting the encapsulated microparticles. Of note, cells encapsulated in such bioencapsulation
30
31 system showed enhanced metabolic activity, and proliferation compared to cells encapsulated
32
33 in non-liquefied alginate hydrogels or in liquefied capsules without microparticles^[4].
34
35 Here, we intend to boost the liquefied and multilayered capsules concept towards their clinical
36
37 application by proposing a high rate production method. Additionally, we aim to design
38
39 capsules with a bioactive outer membrane, which would present cell adhesive properties and
40
41 allow to improve the agglomeration and integration of microcapsules within the surrounding
42
43 tissue. **Figure S1** shows a schematic representation of the production of the multilayered and
44
45 liquefied microcapsules, and the experimental design of the present study.
46
47 Electrohydrodynamic atomization (EHDA) principles were applied to produce microcapsules.
48
49 Then, a multilayered membrane was produced by the assembly of three polyelectrolytes,
50
51
52
53
54
55
56
57
58
59
60
61
62
63
64
65

1
2
3
4
5
6
7
8
9
10
11
12
13
14
15
16
17
18
19
20
21
22
23
24
25
26
27
28
29
30
31
32
33
34
35
36
37
38
39
40
41
42
43
44
45
46
47
48
49
50
51
52
53
54
55
56
57
58
59
60
61
62
63
64
65

namely poly(L-lysine), alginate, and chitosan, by the layer-by-layer (LbL) technique. The last alginate layer was then functionalized with the arginyl-glycyl-aspartic acid (RGD) domain, the most common peptide motif responsible for cell adhesion to the extracellular matrix (ECM). Then, microcapsules were placed on the top of previously formed 2D cell beds composed by HUVECs alone or co-cultured with fibroblasts. Inspired in a concept here termed as 3D+3D, we hypothesized that while within the inside of the liquefied core cells and microparticles would interact and create 3D microstructures, at the same time, microcapsules could interact to create macro 3D structures from the outside. Additionally, upon implantation, the bioactive outer membrane could also improve the microcapsules interaction with the surrounding tissue, contributing to a proper integration and regeneration. This hierarchical 3D macro-and-micro organization should be exclusively cell-mediated. Upon implantation, we envisage that the bio-inspired vascularization substrate provided by the RGD-LbL of microcapsules would promote the recruitment of vessels and other cells involved in the cascade of the regenerative process, promoting tissue healing and integration. Simultaneously, new microaggregates of cells and microparticles could be form inside the microcapsules, which would also contribute to boost the healing process. **Figure 1** summarizes the proposed 3D+3D concept allowing macro-and-micro simultaneous regeneration. The ability of microcapsules to allow cell adhesion on the outer LbL membrane was tested *in vitro*. For that, a cell bed composed by the sequential seeding of human fibroblasts and human umbilical vein endothelial cells (HUVECs) was developed. The combination of the cell bed and the microcapsules system is here termed as microcapsule³. Microcapsules cultured only with HUVECs (microcapsule²) or alone (microcapsule¹) were used as controls. As a *proof-of-principle*, MC3T3-E1 cells were encapsulated with surface modified poly(ϵ -caprolactone) (PCL) microparticles. Cell migration, proliferation, and differentiation were evaluated *in vitro* up to 21 days post-encapsulation. The pro-angiogenic ability of the system was also tested *in ovo* using the chick chorioallantoic membrane (CAM) assay.

2. Results

2.1. Optimum conditions for the production of spherical microgels

To assess the optimum conditions for the production of microgels with the desired morphology and size, an alginate solution was electrosprayed under different flow rates (30, 40, 50, and 60 mL.h⁻¹), polymer concentrations (1.5 and 2% w/v), distances between the tip to the collector (TTC 6, 7, and 8 cm), and applied voltages (10, 15, and 20 kV). A library of microgels with varying morphologies and sizes was obtained. **Figure 2A** shows representative images of the optimization process (constant parameters: 50 mL.h⁻¹, 2% w/v, 6 cm, and 10 kV) and a schematic representation of the EHDA set-up. The comprehensive understanding of the fundamentals of the EHDA process is well-described elsewhere.^[9,10] Our findings showed that the size of the microgels decreased as the polymer concentration increased. Additionally, below 2% w/v the microgels shifted from a circular morphology to a tear-like one. The stability of the jetting mode is highly affected by the voltage and the flow rate. Therefore, by controlling these two parameters monodisperse microgels can be obtained. For flow rates below 30 mL.h⁻¹ and applied voltages above 10 kV, polydisperse microgels were obtained (Figure 2A arrows). Higher flow rates also allowed to obtain microgels in a high-throughput fashion, which was a key factor in the optimization strategy implemented, since the obtained microgels were templates for the production of a cell encapsulation system composed by liquefied microcapsules. At a stable jetting mode, higher flow rates led to the formation of microgels with increased diameters. On the other hand, increasing the TTC distance decreased the strength of the electrical field, and thus higher and/or polydisperse microgels were obtained (Figure 2A arrows). Another key parameter influencing the EHDA process is the solution conductivity. Therefore, when microparticles were loaded into the alginate solution, the EHDA was affected, as shown in Figure 2B2. Therefore, in order to obtain spherical microgels the concentration of alginate was increased to 2.25% w/v. Then, by varying the TTC, microgels encapsulating

1 spherical microparticles (Figure 2B3) with an average diameter of $50 \pm 9 \mu\text{m}$ (Figure 2B4) were
2 obtained. As evidenced in Figure 2B5, monodisperse and circular microgels encapsulating
3 microparticles could be obtained after increasing the TTC distance from 6 cm, optimized for
4 empty microgels, to 8 cm. At 7 cm, although spherical microgels could be obtained, the sample
5 was heterogeneous (Figure 2B5 arrow). Below 7 cm and above 8 cm, microgels presented a
6 tear-like morphology. After the production of the multilayered membrane, microcapsules were
7 immersed in EDTA to liquefy the alginate core. Consequently, the microparticles dispersed in
8 the crosslinked alginate matrix of the spherical microgels (**Figure S2A**), agglomerate at the
9 bottom of the spherical microgels (Figure S2B).
10
11
12
13
14
15
16
17
18
19
20
21
22
23

24 **2.2. 2D cell bed and microcapsules set-up**

25 Microcapsules encapsulating surface modified microparticles and cells were successfully
26 produced, and visualized by LSCM after overnight incubation at 37°C in a humidified air
27 atmosphere of 5% CO_2 . The distribution of the encapsulated cells within the liquefied core of
28 microcapsules was tracked by DAPI nuclei staining (**Figure 3A** blue spots). Importantly, after
29 the EHDA process, the encapsulated cells remained alive, and therefore the parameters of the
30 process, did not jeopardize cell viability (Figure 3B). Prior to the transfer of microcapsules, the
31 last step of the sequential seeding, the engineered cellular environment on the outside
32 environment of microcapsules, termed as cell bed, was evaluated. For that, HUVECs were
33 stained with DiL and their morphology and expression of CD31 was assessed when cultured
34 alone or in a co-culture with fibroblasts (Figure 3C and 3D). As shown, HUVECs-DiL in the
35 co-culture aligned within the extracellular matrix of fibroblasts and presented a more elongated
36 morphology compared to the mono-culture. Additionally, a higher expression of CD31 could
37 be found in the co-culture. To assess the co-localization of the different cells within the triple
38 co-culture system, each cell phenotype was previously stained with a lipophilic dye, namely
39 with DiO, DiL, and DiD for fibroblasts, HUVECs, and MC3T3-E1, respectively. As shown,
40
41
42
43
44
45
46
47
48
49
50
51
52
53
54
55
56
57
58
59
60
61
62
63
64
65

1 MC3T3-E1 encapsulated within the liquefied core of microcapsules are localized at the top of
2 the cell bed composed by fibroblasts and HUVECs (Figure 3E). Interestingly, HUVECs and
3
4 fibroblasts co-exist within the same plane, as shown in Figure 3E zx and zy, showing that
5
6 HUVECs occupied the space left by fibroblasts. Additionally, the alignment of HUVECs within
7
8 the fibroblasts extracellular matrix is observed in Figure 3E xyz. Interestingly, in Figure 3E zx
9
10 and zy fibroblasts and HUVECs could already be detected adhered to the microcapsules,
11
12 although the majority still remained at the bottom of microcapsules, showing that cells migrated
13
14 from the 2D environment towards the 3D structure of microcapsules.
15
16

17
18
19 Microcapsules with an alginate last layer lacking the RGD motif were also produced to assess
20
21 if the previously formed 2D cell beds were able to adhere to the surface of such microcapsules.
22
23 For that, microcapsules composed by a multilayered membrane ending in the poly(L-lysine)
24
25 polyelectrolyte were produced. Poly(L-lysine) is widely used as a coating material known to
26
27 favor cell adhesion. However, HUVECs alone or co-cultured with fibroblasts remained adhered
28
29 to the 2D surface and thus did not migrated towards the multilayered membrane of
30
31 microcapsules (**Figure S3**). Through the transparent core of the liquefied microcapsules, it is
32
33 possible to observe that in the 2D cell bed composed by HUVECs alone, cells presented a
34
35 rounded morphology (Figure S3A), contrary to the stretched morphology observed for the 2D
36
37 cell bed composed by fibroblasts and HUVEC (Figure S3B).
38
39
40
41
42
43
44
45
46
47
48
49
50

51 **2.3. *In vitro* bioperformance**

52
53 The ability of microcapsules to perform as a dual micro-carrier system for tissue engineering
54
55 was assessed. The ability of microcapsules to support living cell encapsulation was assessed up
56
57 to 21 days post-encapsulation. Cell viability and proliferation were evaluated by MTS (**Figure**
58
59 **4A**) and DNA (Figure 4B) quantification assays, respectively. Different microcapsule
60
61
62
63
64
65

1 formulations cultured in basal (bas) or osteogenic differentiation (osteo) media were tested,
2 namely (i) microcapsule³ - microcapsules encapsulating MC3T3-E1 and containing a co-culture
3 of fibroblasts and HUVECs adhered to the external membrane, (ii) microcapsule² -
4 microcapsules encapsulating MC3T3-E1 and containing HUVECs adhered to the external
5 membrane, and (iii) microcapsule¹ - microcapsules encapsulating MC3T3-E1 without cells on
6 the external environment. Of note, MTS and DNA assays were quantified after transferring the
7 samples in order to exclude the contribution resultant from the activity of cells that did not
8 adhere to the membrane of microcapsules. For all the timepoints tested, microcapsule³ presented
9 the highest metabolic activity levels, and microcapsule¹ the lowest. With time, MTS values
10 increase evidencing the ability of microcapsules to support living cell encapsulation.
11 Microcapsules cultured in bas or osteo media presented similar metabolic activity. Regarding
12 the ability of cells to proliferate (Figure 4B), at day 1 no significative differences were found
13 between all the formulations tested. At day 3, such differences began to appear, with
14 microcapsules³ and microcapsules² presenting the highest values compared to microcapsule¹.
15 The higher DNA content of microcapsule³ at days 14 and 21 post-encapsulation, can be
16 explained by the adhesion of fibroblasts and HUVECs to the membrane. Likewise,
17 microcapsules² presented a higher DNA content compared to microcapsule¹, which could also
18 have occurred due to the adhesion of HUVECs. However only a slight increase could be
19 detected. When cultured in the external environment of capsules alone, HUVECs presented a
20 rounded morphology and a poor migrating ability compared to the co-culture with fibroblasts.
21 In fact, the adhesion of HUVECs to the membrane could hardly be detected, presenting a high
22 similarity to microcapsule¹ (**Figure S4**). Contrarily, cells in the external co-culture environment
23 were able to adhere to the membrane of microcapsules (Figure 4D), and after overnight
24 incubation cell were able to migrate from the 2D cell bed to the 3D environment provided by
25 microcapsules (Figure 4D squares). With time, macroaggregates composed by the assembling
26 of microcapsules could be detected (Figure 4E and 4H). These macroaggregates were cell-

1 mediated by the action of fibroblasts and HUVECs, which started to migrate from the cell
2 network towards the membrane of the microcapsules that after 8h of incubation (Figure 4F and
3
4 4I). This behavior occurred independently from the cell culture media used, whether bas or
5
6 osteo media. While macroaggregates were formed due to the agglomeration of microcapsules,
7
8 encapsulated cells simultaneously formed microaggregates by recruiting the co-encapsulated
9
10 microparticles (Figure 4G and 4J, and **Figure S4**). Therefore, the proposed system allowed the
11
12 simultaneous creation of cell-mediated macro (by agglomerating microcapsules) and micro (by
13
14 agglomerating microparticles) aggregates. Additionally, the encapsulated cells were able to
15
16 undergo cell differentiation towards the osteogenic lineage, as shown by the quantification of
17
18 the activity of alkaline phosphatase (ALP) (Figure 4C). Of note, ALP activity peaks occurred
19
20 at later timepoints, namely at days 14 and 21 post-encapsulation, but only when microcapsules
21
22 were cultured in osteogenic differentiation medium.
23
24
25
26
27
28
29
30

31 **2.4. Angiogenic potential**

32
33 The angiogenic potential of microcapsules was assessed after *in ovo* implantation using the
34
35 CAM assay (**Figure 5**). Remarkably, results show that microcapsules were able to recruit a
36
37 similar number of new microvessels compared to CAMs without microcapsules and
38
39 supplemented with basic fibroblast growth factor-2 (bFG-2, control +). Since microcapsules
40
41 were transferred to the CAM model in serum free α -MEM, a negative control of CAMs
42
43 supplemented with culture medium was also used (control -). The number of microvessels
44
45 recruited by microcapsules was significantly higher compared to control -, evidencing that such
46
47 differences were prompt by the microcapsule system itself, due to their functionalized RGD
48
49 LbL membrane. Of note, only microvessels with a diameter below 20 μ m were considered for
50
51 the quantification. Microvessels were quantified in a well-defined Region of Interest (ROI) for
52
53 all conditions. The new vascular network formed within the ROI was similar to the vascular
54
55 network formed by the control+ environment, in terms of the number of junctions (Figure 5D),
56
57
58
59
60
61
62
63
64
65

1 although no significative differences were found for both conditions compared to control-.
2 Additionally, microcapsules prompted the formation of a vascular network composed by
3 vessels with increased lengths compared to the control-.
4
5
6
7
8
9

10 **3. Discussion**

11 Liquefied and multilayered capsules have emerged as an alternative bioencapsulation system
12 in which cells and microparticles are encapsulated in a liquefied environment. The system is
13 composed by four main components, each one with specific functions, namely (i) a
14 permselective multilayered membrane, (ii) microparticles, (iii) cells, and (iv) a liquefied core.
15 The membrane is composed by chitosan, poly(L-lysine), and alginate electrostatically
16 interacting by the LbL technique. It acts as a physical barrier that mediates the interaction
17 between the inside and outside environment of capsules, thus avoiding the entrance of large
18 molecules and other cells, while ensuring the permeability of essential molecules for long-term
19 cell survival. Microparticles provide adhesion sites required for different biological processes
20 of anchorage-dependent cells, both dispersed in the liquefied core. We already demonstrated
21 the superior biological performance of liquefied and multilayered microcapsules co-
22 encapsulating cells and microparticles when compared to classical alginate hydrogels or with
23 liquefied and multilayered microcapsules without microparticles^[4]. Results showed that the
24 system presented an enhanced metabolic activity, cell viability, and proliferation up to 28 days
25 of *in vitro* culture. Cells and microparticles, encapsulated within the privilege liquefied
26 environment of capsules can move freely, and macroaggregates containing cells and
27 microparticles could be visualized by SEM or by fluorescence microscopy after F-actin
28 staining. We believe that the established concept of liquefied and multilayered capsules as
29 bioencapsulation system for regenerative medicine can find great applicability and value when
30 used as building blocks to create complex 3D structures with clinical relevance. Therefore, we
31 herein intend to take the concept of liquefied and multilayered capsules a step further by
32
33
34
35
36
37
38
39
40
41
42
43
44
45
46
47
48
49
50
51
52
53
54
55
56
57
58
59
60
61
62
63
64
65

proposing the combination of the high rate production of EHDA with the versatility and ease of the LbL technique to modify 3D structures. EHDA applied to produce cell encapsulation systems is often called bioelectrospraying (BES). Due to the low current of BES, the process enables to produce cell encapsulation systems with high cell viability. Xin *et al.*^[11] showed that up to 15 kV and a TTC of 15 cm, the viability and proliferation of six different cell types was not affected. Additionally, BES has also reported to do not affected the multilineage differentiation ability of mesenchymal stromal cells (MSCs).^[12] Herein, we used the BES technique to not only encapsulate cells but also microparticles. We optimized the parameters of the process to present the simplest set-up, rather than increasing its complexity by applying coaxial needles, high voltages or sheath gas.^[13] The proposed BES set up allowed to produce a library of spherical beads at high rates presenting different diameters (Figure 2). The rationale to select the optimized BES parameters to produce the hydrogel templates was a circularity close to 1 at the lowest voltage and highest flow rate, due to cell viability and scale-up concerns, respectively. Once the spherical hydrogels were obtained, a multilayered membrane was built by LbL technique. We have been employing this low cost and versatile technique to modify or construct 3D tissue engineering systems.^[7,14–17] Taking advantage of the versatility of the LbL technique, we conferred cell adhesion capability to the multilayered membrane simply by changing one of the polyelectrolyte solutions. Previously, we have reported the superior stability and an exponential regime growth of the multilayered membrane when combining three-polyelectrolytes, namely poly(L-lysine), chitosan, and alginate, compared to the classical two-system.^[4] Here, alginate combined with the well-known peptide sequence RGD was used to modify the last layer of the multilayered membrane of microcapsules. Our goal was to propose a dual-building block system by exploring the ability of microcapsules to produce microaggregates of cells and microparticles within the liquefied core, while at the same time, microcapsules could be assembled by cells and create macro and more complex 3D structures. Our *in vitro* results show the successful production and bioperformance of such system. The

1 superior organization of HUVECs when placed in a co-culture with fibroblasts (Figure 3D) was
2 attributed to the ability of the later to provide important factors that modulate the growth and
3 stability of capillary sprouts.^[18] Not limited to fibroblasts, other studies have also achieved
4 tubular endothelial cell networks by co-culturing HUVECs with mesenchymal stromal cells.^[19]
5
6 The production of microcapsules does not jeopardize cell viability, since cells remain
7 metabolically active (Figure 4A) up to 21 days post-encapsulation. Additionally, cells are able
8 to proliferate (Figure 4B). We also demonstrated that if desired, the encapsulated cells could
9 undergo lineage differentiation (Figure 4C). However, peaks of ALP activity were only
10 expressed when microcapsules were cultured in osteogenic differentiation medium. Previously,
11 we reported that adipose-derived stromal cells encapsulated in liquefied and multilayered
12 capsules could differentiate towards the osteogenic lineage in the absence of two major
13 supplemental osteogenic differentiation factors, namely dexamethasone and ascorbic.^[7,8] Cell
14 differentiation was prompted by the crosstalk of biomolecules, namely BMP-2 released by
15 endothelial cells, when both cells were co-encapsulated within liquefied and multilayered
16 capsules. Similarly, endothelial cells released VEGF, which could be detected on the outside
17 environment of capsules, and thus the system was also validated to act as a release system of
18 biomolecules. However, here such event did not occur since pre-osteoblastic cells and HUVECs
19 were not co-encapsulated, and thus they were not in direct contact. The presence of the LbL
20 membrane between these two cell phenotypes inhibited the formation of the gap junction
21 connexin 43, a predominant gap junction protein in osteoblasts. Several studies demonstrate the
22 ability of connexin 43 to form gap junctions between endothelial and osteogenic cells in direct
23 co-culture.^[20–25] Of note, although the system has been validated for bone and cartilage
24 regeneration, the modular ability of the liquefied microcapsules widely opens their applicability
25 for different tissue engineering strategies. Either by changing the type of cells and
26 microparticles encapsulated, or the type of functionalization employed to the multilayered
27 membrane, a plethora of different cell encapsulation systems can be formulated. Besides
28
29
30
31
32
33
34
35
36
37
38
39
40
41
42
43
44
45
46
47
48
49
50
51
52
53
54
55
56
57
58
59
60
61
62
63
64
65

1 simultaneously conferring macro (Figure 4E and 4H) and micro (Figure 4G, 4J and S4) cell-
2 mediated aggregation, liquefied and multilayered microcapsules also presented angiogenic
3 ability, demonstrated *in ovo* using the CAM model (Figure 5). The pro-angiogenic ability of
4 microcapsules conferred by the RGD-LbL membrane prompted an angiogenic response similar
5 to that observed when CAMs were supplemented with bFGF-2 (control+). This observation is
6 supported by the similar number of microvessels that were recruited in microcapsules and
7 control+ (Figure 5D). Additionally, geometrical parameters of the vasculature formed were also
8 analyzed, namely the number of junctions and the branch length. The vasculature observed in
9 microcapsules and control+ presented higher lengths compared to control -, which increases the
10 possibility of branching to occur. We envisage that upon implantation *in vivo*, the proposed
11 microcapsules would stimulate the recruitment of blood vessels. Angiogenic capacity of
12 biomaterials is a key asset to attain full tissue functionality, not only due to the transport of
13 essential molecules for cell survival but also to allow a proper tissue integration.^[26]

14 The promising results obtained, makes us to believe that the proposed system once implanted
15 would easily adapt to lesions with complex shapes, and recruit new vessels while also
16 interacting with other cells involved in the cascade of the regenerative process. While aiding
17 from the outside the healing of the tissue, on the inside, the new microaggregates of cells and
18 microparticles formed would contribute to accelerate the process.

49 **4. Experimental Section**

50 *Microparticles production and surface functionalization:* Poly(ϵ -caprolactone) (PCL)
51 microparticles were produced by oil/water (o/w) emulsion technique, and surface modified by
52 combining plasma treatment with collagen I as similarly described in our previous study.^[4] PCL
53 (5% w/v, M_n 80,000, Merck) was dissolved in methylene chloride (CH_2Cl_2 , Honeywell Riedel-

1 de Haën™). Under agitation, this solution was added to polyvinyl alcohol (0.5%, PVA, Merck).
2 After 2 days at RT, the produced microparticles were subsequently collected, washed with
3 distilled water, and dried in ethanol. Microparticles were then placed in a plasma reactor
4 chamber (ATTO, Diener Electronic) fitted with a radio frequency generator. Air was used as
5 the working atmosphere. A glow discharge plasma (0.4 mbar, 30 V) was created for 15 min.
6 Subsequently, microparticles (500 mg) were sterilized in 70 % v/v ethanol, and immersed in
7 collagen (1200 µg, type I solution from rat tail, Merck) diluted in acetic acid (0.02 M) at 4°C
8 overnight. The diameter of microparticles was measured by *ImageJ* software.
9
10
11
12
13
14
15
16
17
18
19
20
21

22 *2D cell beds:* Human fibroblasts (primary dermal fibroblasts, PCS-201-012, ATCC) were
23 cultured in DMEM-high glucose (ThermoFisher Scientific) supplemented with FBS (10 % v/v,
24 ThermoFisher Scientific) and antibiotic-antimycotic (1% v/v, ThermoFisher Scientific). At
25 ~80% confluency, cells were detached using trypsin-ethylenediaminetetraacetic acid (EDTA)
26 (Merck) at 37°C for 5 min. After 5 min of centrifugation at 300 g, the supernatant was discarded.
27 Cells (10,000 cells per well) were suspended in culture medium and seeded in µ-slide 8 wells
28 (ibidi). After 48h of incubation 37°C in a humidified atmosphere composed of 5% CO₂,
29 HUVECs (10,000 cells per well) were placed on top of fibroblasts. For that, HUVECs (PCS-
30 100-010, ATCC) cultured in M199 supplemented with FBS (20 % v/v), antibiotic-antimycotic
31 (1% v/v), GlutaMAX (1% v/v, ThermoFisher Scientific), heparin sodium salt from porcine
32 intestinal mucosa (180U, 10 mg.mL⁻¹, Merck), and endothelial cell growth supplement (Merck),
33 were detached using trypsin-EDTA (Merck) at 37°C for 5 min. After 5 min of centrifugation at
34 300 g, the supernatant was discarded. Fibroblasts co-cultured with HUVECs were incubated in
35 supplemented DMEM-high glucose and M199 (1:1). HUVECs were also cultured alone
36 (10,000 cells per well) in supplemented M199 medium. After 48h of HUVECs seeding,
37 liquefied and multilayered microcapsules were placed on top of 2D cell beds.
38
39
40
41
42
43
44
45
46
47
48
49
50
51
52
53
54
55
56
57
58
59
60
61
62
63
64
65

Liquefied and multilayered microcapsules: MC3T3-E1 cells (Subclone 4, ATCC CRL-2593) were cultured in Gibco® MEM α (ThermoFisher Scientific) supplemented with fetal bovine serum (FBS, 10 % v/v, ThermoFisher Scientific) and antibiotic-antimycotic (1% v/v, ThermoFisher Scientific). At ~80% cells were detached using trypsin-EDTA at 37°C for 5 min. After 5 min of centrifugation at 300 g, the supernatant was discarded. Cells were suspended in a solution containing sodium alginate (2.5 % w/v, W201502, Merck), sodium chloride (0.15 M, NaCl, LabChem), and MES hydrate (25 mM, Merck) at pH 6.7. Alginate microgels encapsulating cells ($1 \times 10^6 \cdot \text{mL}^{-1}$) and microparticles ($30 \text{ mg} \cdot \text{mL}^{-1}$) were obtained by EHDA at 10 kV, 8 cm, and 50 mL.h⁻¹ (total infused: 10 mL alginate). Prior to cell encapsulation, empty alginate microgels were also obtained for optimization procedures. For that, EHDA was tested using variable alginate concentrations (1.5 and 2% w/v), voltage (10, 15, and 20 kV), and distances between the tip to the collector (TTC, 6, 7, and 8 cm). All microgels were collected in a stirring calcium chloride bath (0.1 M, Merck) buffered with MES hydrate (25 mM, Merck) at pH 7. After 15 min at RT, microgels were collected and rinsed in a washing solution of NaCl (0.15 M). The layer-by-layer membrane was obtained by subsequent adsorption of oppositely charged polyelectrolytes, namely first in poly(L-lysine) (M_n 30,000-70,000, pH 7, Merck), followed by peptide-coupled alginate (MVG GRGDSP, pH 7, Novatrix), water-soluble chitosan (pH 6, Protasan UP CL 213, NovaMatrix), and, ultimately, in peptide-coupled alginate again. The polyelectrolyte solutions ($0.3 \text{ mg} \cdot \text{mL}^{-1}$) were dissolved in NaCl (0.15 M) containing MES hydrate (25 mM). Following 10 min of immersion for each polyelectrolyte, non-adsorbed macromolecules were removed by NaCl (0.15 M) rinsing. This process was repeated three times in order to obtain a 10-layered membrane. Microgels with a 9-layered membrane ending in the poly(L-lysine) polyelectrolyte were also produced (control). The coated microgels were immersed in EDTA (20 mM, Merck) at pH 7 for 3 min to liquefy the alginate core. Ultimately, microcapsules were suspended in supplemented Gibco® MEM α (20 mL) and transferred (150 μL per well) to the μ -slide 8 wells containing the 2 cell beds with (*i*) fibroblast co-cultured with

1 HUVECs (microcapsules³), or (ii) HUVECs (microcapsules²). Microcapsules were also
2 transferred to wells without 2D cell beds (microcapsules¹). All microcapsules were cultured in
3
4 Gibco® MEM α supplemented with 10 % v/v FBS and 1% v/v antibiotic-antimycotic, here
5
6 termed as basal medium (bas), or in Gibco® MEM α supplemented with FBS (10 % v/v),
7
8 antibiotic-antimycotic (1% v/v), ascorbic acid (50 $\mu\text{g}\cdot\text{mL}^{-1}$, Merck), and β -glycerophosphate
9
10 (10 mM, Merck), here termed as osteogenic differentiation medium (osteo).
11
12
13
14
15

16
17 *Lipophilic dyes fluorescent labeling:* Fibroblasts, HUVECs, and MC3T3-E1 were stained with
18
19 lipophilic dyes 3,3'-dioctadecyloxycarbocyanine perchlorate (DiO, green), 1,1'-dioctadecyl-
20
21 3,3,3',3'-tetramethylindocarbocyanine perchlorate (DiL, red), and 1,1'-dioctadecyl-
22
23 3,3,3',3'-tetramethylindodicarbocyanine, 4-chlorobenzenesulfonate salt (DiD, blue),
24
25 respectively. Cells were incubated with each dye (1mL containing 2 μM per 1×10^6 cells) at 37°C
26
27 for 15 min. Labeled cells were then used to construct the microcapsules³ system, and visualized
28
29 by laser scanning confocal microscopy (LSCM, LSM 510 META, Zeiss).
30
31
32
33
34
35

36
37 *Metabolic viability-based assay:* the mitochondrial metabolic activity of the encapsulated cells
38
39 was measured using the CellTiter 96® AQueous One Solution Cell Proliferation Assay
40
41 (Promega). At 1, 3, 7, 14, and 21 days post-encapsulation, microcapsules were aspirated and
42
43 transferred to 1 mL centrifuge tubes. Following centrifugation at 300 g for 5 min, the
44
45 supernatant was discarded and samples were suspended in PBS containing 3-(4,5-
46
47 dimethylthiazol-2-yl)-5-(3-carboxymethoxyphenyl)-2-(4-sulphophenyl)-2H-tetrazolium (MTS,
48
49 1:6, 500 μL). After 4h of incubation at 37°C, 100 μL of each well (in quadruplicate) were
50
51 transferred to a 96-well plate. The amount of formazan product was measured by absorbance at
52
53 a wavelength of 490 nm using a multiwall spectrophotometer (Synergy HTX, Biotek).
54
55
56
57
58
59
60
61
62
63
64
65

1
2
3
4
5
6
7
8
9
10
11
12
13
14
15
16
17
18
19
20
21
22
23
24
25
26
27
28
29
30
31
32
33
34
35
36
37
38
39
40
41
42
43
44
45
46
47
48
49
50
51
52
53
54
55
56
57
58
59
60
61
62
63
64
65

Total dsDNA quantification and alkaline phosphatase activity (ALP): Total dsDNA quantification was performed using the assay kit Quant-iT™ PicoGreen® (Life Technologies). Samples were aspirated and transferred to 1 mL centrifuge tubes. Following centrifugation at 300 g for 5 min, the supernatant was discarded and samples were suspended in ultra-pure sterile water (1 mL per sample) for cell lysis. After 1 h in a 37°C shaking water bath, samples were frozen at -80°C at least overnight. Samples were defrosted and used according to the specifications of the kit. A standard curve for DNA analysis was generated with the provided dsDNA solution. After 10 min of incubation at RT, fluorescence was read at an excitation wavelength of 485/20 nm and 528/20 nm of emission using a microplate reader (Gen 5, Synergy HTX, Biotek). Samples resultant from cell lysis were also used for the quantification of the activity of alkaline phosphatase. A substrate solution (pH 9.8) was prepared by dissolving 4-nitrophenylphosphate disodium salt hexahydrate (0.2 % w/v, Merck) in diethanolamine (1 M, Sigma-Aldrich). Each sample (20 µL, in triplicate) was mixed with the prepared substrate solution (60 µL). After 45min at 37°C protected from light, the reaction was stopped (80 µL) with sodium hydroxide (2 M) and EDTA (0.2 mM). A standard curve with a range of concentrations was prepared by diluting 4-nitrophenol solution (10 mM, Merck) in the stop solution. Absorbance was read at 405 nm in a microplate reader (Synergy HTX, Biotek). Statistical analysis was performed using two-way analysis of variance (ANOVA) with Tukey's post-hoc test (GraphPad Prism 6.0). A p-value <0.05 was considered statistically significant. Only non-significant differences (ns) were marked to facilitate the interpretation of the data. All results are presented as mean ± SD.

Scanning Electron Microscopy (SEM): Microcapsules were fixed at RT in formalin (10% v/v) for 30 min, and subsequently dehydrated in increasing gradient series of ethanol (10 min each). The membrane of microcapsules was destroyed to expose the core contents. After gold sputtering, samples were visualized (25 kV, S4100, Hitachi).

1
2
3
4
5
6
7
8
9
10
11
12
13
14
15
16
17
18
19
20
21
22
23
24
25
26
27
28
29
30
31
32
33
34
35
36
37
38
39
40
41
42
43
44
45
46
47
48
49
50
51
52
53
54
55
56
57
58
59
60
61
62
63
64
65

CD31 immunofluorescence staining of 2D cell beds: Following 48h of HUVECs seeding, 2D cell beds were fixed in formalin (10% v/v) for 30 min at RT, and permeabilized for 5 min at RT with Triton X-100 (0.1% v/v, Merck). Prior to cell seeding, HUVECs were labelled with DiL (1mL containing 2 μ M per 1x10⁶ cells) at 37°C for 15 min. 2D cell beds composed by fibroblasts co-cultured with HUVECs-DiL or HUVECs-DiL alone were then immersed in FBS/PBS (5% w/v) for 1 h at RT to block non-specific binding, and then incubated overnight at 4°C with the primary antibody mouse anti-human CD31 (Biolegend, 1:100 in 5% FBS/PBS). After PBS washing, samples were incubated for 1h at RT with the secondary antibody anti-mouse AlexaFluor 488 (Biolegend, 1:500 in 5% FBS/PBS). After PBS washing, samples were counterstained with 4',6-diamidino-2-phenylindole, dihydrochloride (DAPI, 1 mg.mL⁻¹ diluted 1:1000 in PBS, ThermoFisher Scientific) for 5 min at RT, and analyzed by fluorescence microscopy (Axio Imager 2, Zeiss).

F-actin filaments fluorescence staining: Microcapsules were fixed at RT in formalin (10% v/v) for 30 min, and permeabilized for 5 min at RT with Triton X-100 (0.1% v/v). Samples were stained with phalloidin (Flash Phalloidin Red 594, 1:40 in PBS, Biolegend) for 45 min at RT, and then counterstained with DAPI (1 mg.mL⁻¹ diluted 1:1000 in PBS) for 5 min at RT. Microcapsules were analyzed by fluorescence microscopy (Axio Imager 2, Zeiss).

Calcein-AM fluorescence staining: Microcapsules encapsulating MC3T3-E1 and PCL microparticles stained with Nile red were immersed in a PBS (1 mL) solution containing Calcein-AM (1 μ L) for 15 min at 37°C. After PBS washing, samples were immediately visualized by fluorescence microscopy (Axio Imager 2, Zeiss).

Chick chorioallantoic membrane (CAM) assay: The CAM assay was used to evaluate the angiogenic response of microcapsules. After EHDA production, microcapsules (total infused:

10 mL alginate) were incubated at 37°C and 5% CO₂ in serum-free Gibco® MEM α (20 mL) supplemented with antibiotic-antimycotic (1% v/v). After an overnight incubation, microcapsules were implanted in fertilized chicken (*gallus gallus*) eggs, obtained from commercial sources, which were previously incubated horizontally at 37.8 °C in a humidified atmosphere for 10 days. A square window was opened in the shell after removal of 2–2.5 mL of albumen, to allow detachment of the developing CAM. The window was sealed with adhesive tape and the eggs returned to the incubator. Microcapsules (20 μ L) were transferred to a 3 mm silicone ring under sterile conditions. CAMs without microcapsules and supplemented with basic fibroblast growth factor (bFGF, 500 ng) or with Gibco® MEM α supplemented with antibiotic-antimycotic (1% v/v) were used as positive and negative controls, respectively. The eggs were re-sealed and returned to the incubator for 3 days. After removing the silicone ring, CAMs were excised from the embryos and visualized *ex-ovo* under light microscopy (SZX16 coupled with a DP71 camera, Olympus). The number of new vessels (<20 μ m in diameter) growing radially towards the inoculation site were counted blinded. Statistical analysis was carried out using GraphPad Prism 6 software. Data is presented as mean \pm standard deviation (SD) from 10 eggs (n=3). A using two-way analysis of variance (ANOVA) with Kruskal-Wallis test was used. A p-value <0.05 was considered statistically significant.

Supporting Information

Supporting Information is available from the Wiley Online Library or from the author.

Acknowledgements

The authors acknowledge the funding from the European Research Council (ERC) for project ATLAS (ERC-2014-ADG-669858), and the Portuguese Foundation for Science and Technology (FTC) for project CIRCUS (PTDC/BTM-MAT/31064/2017). This work was

1 developed within the scope of the project CICECO-Aveiro Institute of Materials, FCT Ref.
2 UID/CTM/50011/2019, financed by national funds through the FCT/MCTES. This work was
3
4 also partly supported by Japan Society for the Promotion of Science (JSPS) Bilateral Open
5
6 Partnership Joint Research Projects. The authors are also grateful to A. Sofia Silva (Figure 3A
7
8 and 4D) and Vítor M. Gaspar (Figure 3E) for LSCM imaging. Image acquisition was performed
9
10 in the LiM facility of iBiMED, a node of PPBI (Portuguese Platform of BioImaging) with grant
11
12 agreement number POCI-01-0145-FEDER-022122.
13
14

15
16
17 Received: ((will be filled in by the editorial staff))

18 Revised: ((will be filled in by the editorial staff))

19 Published online: ((will be filled in by the editorial staff))
20
21
22

23 References

24
25
26

- 27 [1] C. R. Correia, R. L. Reis, J. F. Mano, *Adv. Healthc. Mater.* **2018**, *7*, 1701444.
28
29 [2] J. Li, D. J. Mooney, *Nat. Rev. Mater.* **2016**, *1*, DOI 10.1038/natrevmats.2016.71.
30
31 [3] O.-W. Merten, *Philos. Trans. R. Soc. Lond. B. Biol. Sci.* **2015**, *370*, 20140040.
32
33 [4] C. R. Correia, R. L. Reis, J. F. Mano, *Biomacromolecules* **2013**, *14*, 743.
34
35 [5] C. R. Correia, P. Sher, R. L. Reis, J. F. Mano, *Soft Matter* **2013**, *9*, 2125.
36
37 [6] C. R. Correia, S. Gil, R. L. Reis, J. F. Mano, *Adv. Healthc. Mater.* **2016**, *5*, 1346.
38
39 [7] C. R. Correia, R. P. Pirraco, M. T. Cerqueira, A. P. Marques, R. L. Reis, J. F. Mano,
40
41
42
43
44
45
46
47
48
49
50
51
52
53
54
55
56
57
58
59
60
61
62
63
64
65
Sci. Rep. **2016**, *6*, 21883.
[8] C. R. Correia, T. C. Santos, R. P. Pirraco, M. T. Cerqueira, A. P. Marques, R. L. Reis,
J. F. Mano, *Acta Biomater.* **2017**, *53*, 483.
[9] S. K. Boda, X. Li, J. Xie, *J. Aerosol Sci.* **2018**, *125*, 164.
[10] D. N. Nguyen, C. Clasen, G. Van den Mooter, *J. Pharm. Sci.* **2016**, *105*, 2601.
[11] Y. Xin, G. Chai, T. Zhang, X. Wang, M. Qu, A. Tan, M. Bogari, M. Zhu, L. Lin, Q.
Hu, et al., *Biomed. Reports* **2016**, *5*, 723.

- 1
2
3
4
5
6
7
8
9
10
11
12
13
14
15
16
17
18
19
20
21
22
23
24
25
26
27
28
29
30
31
32
33
34
35
36
37
38
39
40
41
42
43
44
45
46
47
48
49
50
51
52
53
54
55
56
57
58
59
60
61
62
63
64
65
- [12] Z. McCrea, Y. Arnanthigo, S.-A. Cryan, S. O’Dea, *J. Med. Biol. Eng.* **2018**, *38*, 497.
- [13] J. Wang, J. A. Jansen, F. Yang, *Front. Chem.* **2019**, *7*, 258.
- [14] J. Borges, L. C. Rodrigues, R. L. Reis, J. F. Mano, *Adv. Funct. Mater.* **2014**, *24*, 5624.
- [15] J. M. Silva, N. Georgi, R. Costa, P. Sher, R. L. Reis, C. a Van Blitterswijk, M. Karperien, J. F. Mano, *PLoS One* **2013**, *8*, 1.
- [16] S. M. Oliveira, V. E. Santo, M. E. Gomes, R. L. Reis, J. F. Mano, *Biomaterials* **2015**, *48*, 56.
- [17] T. D. Gomes, S. G. Caridade, M. P. Sousa, S. Azevedo, M. Y. Kandur, E. T. Öner, N. M. Alves, J. F. Mano, *Acta Biomater.* **2018**, *69*, 183.
- [18] M. N. Nakatsu, R. C. A. Sainson, J. N. Aoto, K. L. Taylor, M. Aitkenhead, S. Pérez-del-Pulgar, P. M. Carpenter, C. C. W. Hughes, *Microvasc. Res.* **2003**, *66*, 102.
- [19] B. Andrée, H. Ichanti, S. Kalies, A. Heisterkamp, S. Strauß, P.-M. Vogt, A. Haverich, A. Hilfiker, *Sci. Rep.* **2019**, *9*, 5437.
- [20] X. Fan, Y. Teng, Z. Ye, Y. Zhou, W.-S. Tan, *J. Cell Sci.* **2018**, *131*, jcs216135.
- [21] M. C. Moorer, J. P. Stains, *Curr. Osteoporos. Rep.* **2017**, *15*, 24.
- [22] L. I. Plotkin, T. Bellido, *Bone* **2013**, *52*, 157.
- [23] F. Villars, B. Guillotin, T. Amédée, S. Dutoya, L. Bordenave, R. Bareille, J. Amédée, *Am. J. Physiol. Physiol.* **2002**, *282*, C775.
- [24] Y. Chen, M. Chen, T. Xue, G. Li, D. Wang, P. Shang, J. X. Jiang, H. Xu, *J. Cell. Physiol.* **2019**, jcp. 28581.
- [25] B. Guillotin, R. Bareille, C. Bourget, L. Bordenave, J. Amédée, *Bone* **2008**, *42*, 1080.
- [26] N. Mitrousis, A. Fokina, M. S. Shoichet, *Nat. Rev. Mater.* **2018**, *3*, 441.

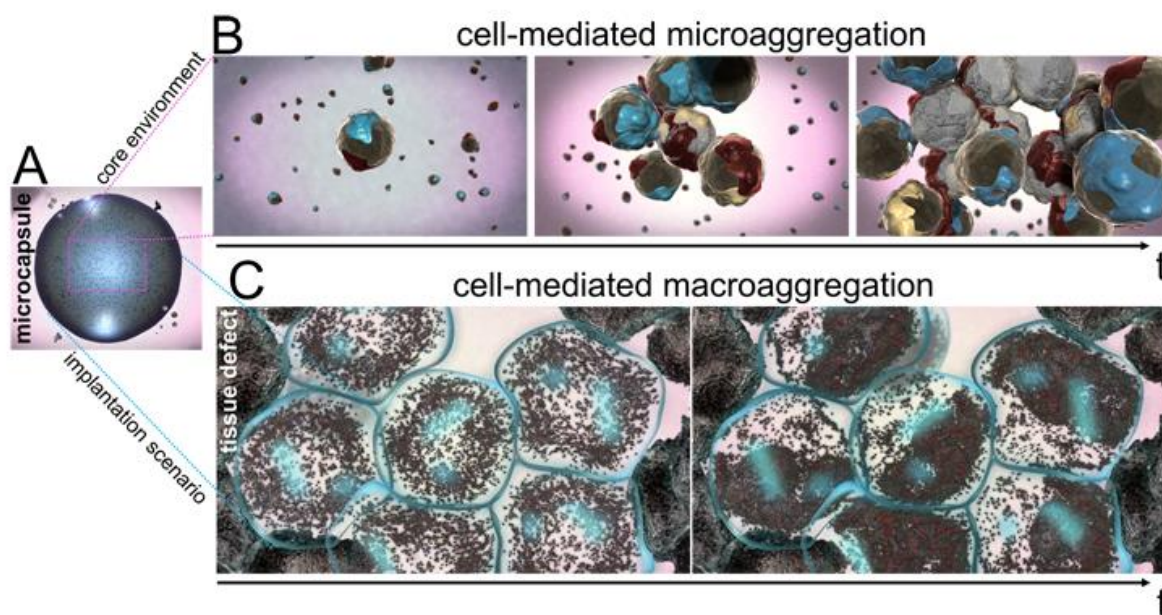


Figure 1 – Schematic representation of the microcapsules system proposed. **(A)** Overview of a liquefied and multilayered capsule composed by a permselective membrane that allows the entrance of essential molecules for cells survival and avoids the entrance of high molecules and other cells. **(B)** Cells and microparticles encapsulated within the liquefied core can move freely. Inside the microcapsules, different cell phenotypes can be combined, and besides proliferation, cells can undergo differentiation. **(C)** After implantation, microcapsules can easily adapt to a tissue defect, and agglomerate to form macrostructures able to fulfil a large defect.

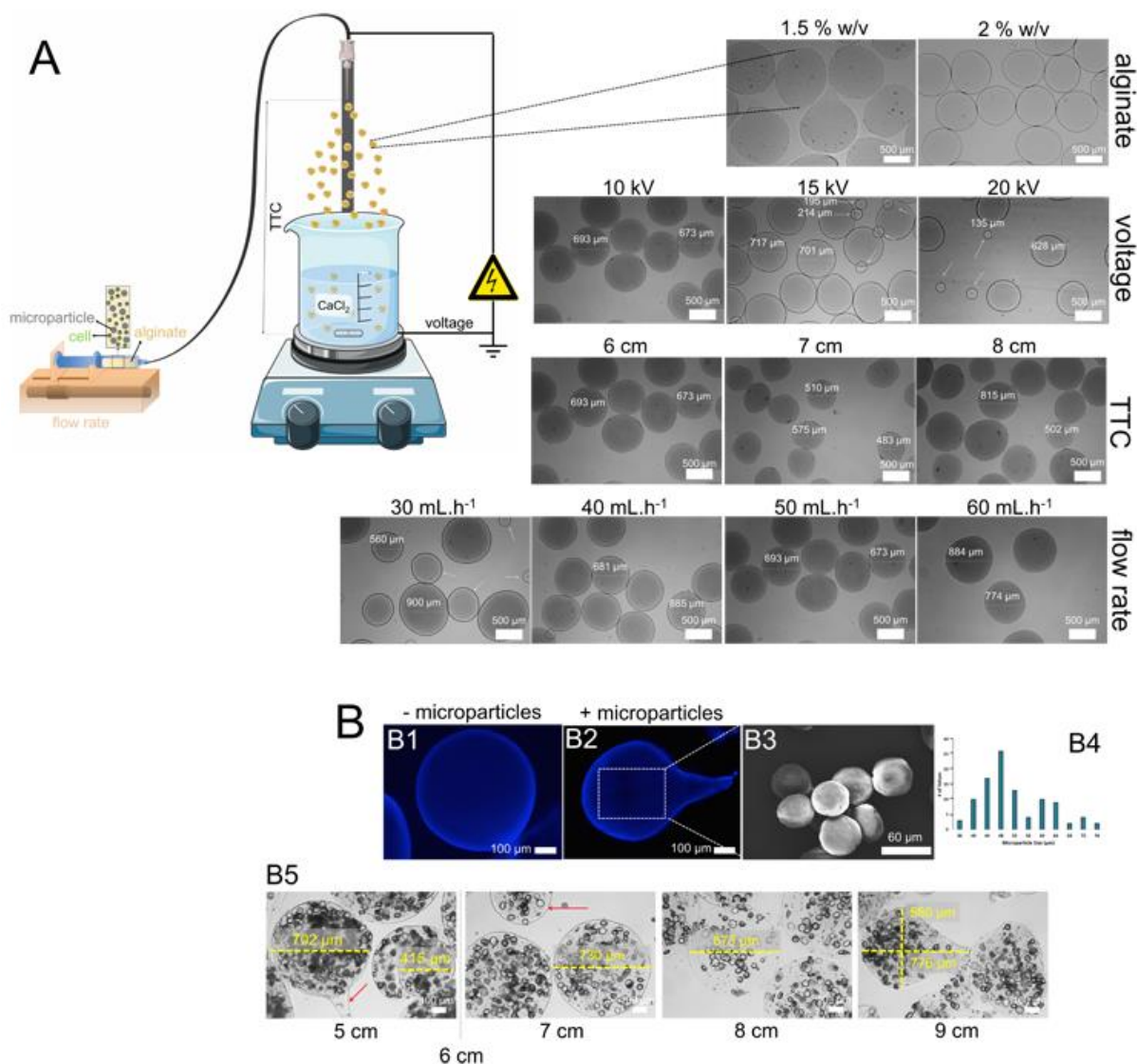


Figure 2 – Representative images of the optimization process to obtain alginate hydrogels by electrohydrodynamic atomization (EHDA). **(A)** Different parameters of the process were tested to obtain empty alginate hydrogels, namely the alginate concentration (% w/v), the flow rate (30, 40, 50, and 60 mL.h⁻¹), the distance between the tip to the collector (TTC 6, 7, and 8 cm), and the applied voltage (10, 15, and 20 kV). Constant parameters: 2% w/v alginate, 50 mL.h⁻¹ flow rate, TTC 6 cm, and 10 kV of applied voltage. **(B)** Optimization of the TTC required to obtain spherical alginate hydrogels containing microparticles. **(B1)** Empty alginate hydrogel produced by EHDA at 2 % w/v, 50 mL.h⁻¹, 6 cm, and 10 kV. **(B2)** Alginate hydrogels encapsulating microparticles produced by EHDA using the same parameters of **(B1)**. **(B3)** SEM image of the polycaprolactone microparticles produced by oil/water emulsion. **(B4)** Histogram

of the diameter frequency of the microparticles. **(B5)** Representative images of the optimization process to obtain alginate hydrogels loaded with microparticles by testing different TTC of the EHDA process using 2.5% w/v alginate, 50 mL.h⁻¹ flow rate, and 10 kV of voltage.

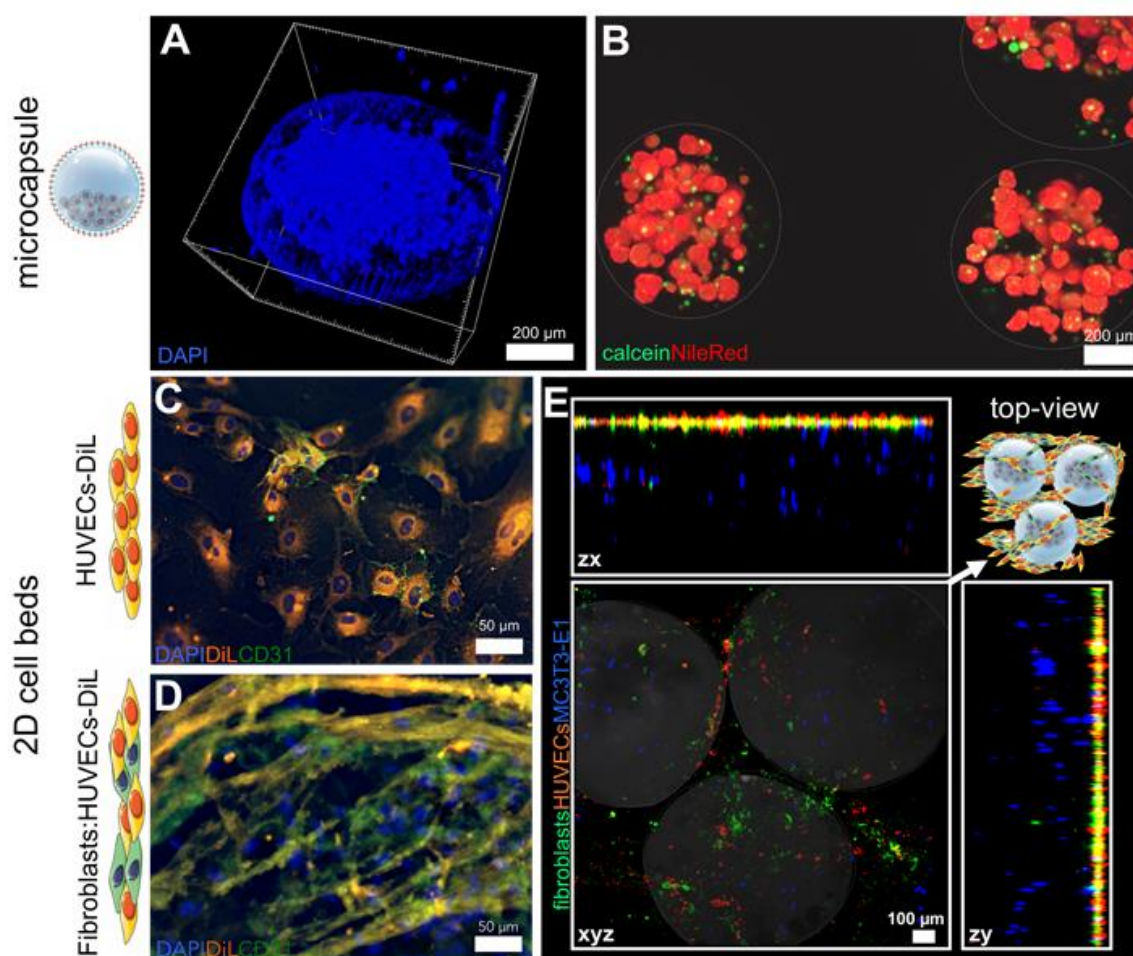


Figure 3 – (A) Overview of a liquefied microcapsule encapsulating MC3T3-E1 cells and polycaprolactone (PCL) microparticles visualized by laser scanning confocal microscopy (LSCM). Cell nuclei was stained with DAPI (blue). Scale bar is 200 µm. (B) Microcapsules encapsulating living MC3T3-E1 cells stained with calcein (green) and PCL microparticles fluorescently marked with Nile Red. Scale bar is 200 µm. (C) Immunofluorescence of CD31 (green) in a 2D co-culture of fibroblast and HUVECs fluorescently marked with DiL (orange).

1 Cell nuclei was stained with DAPI (blue). Scale bar is 50 μm . **(D)** Immunofluorescence of
2 CD31 (green) in a 2D culture of HUVECs fluorescently marked with DiL (orange). Cell nuclei
3
4 was stained with DAPI (blue). Scale bar is 50 μm . **(E)** LSCM of the triple sequential co-culture
5
6 system composed by microcapsules encapsulating MC3T3-E1 cells and PCL microparticles
7
8 localized at the top of a 2D co-culture of fibroblasts and HUVECs. Fibroblasts, HUVECs, and
9
10 MC3T3-E1, were previously stained with DiO (green), DiL (orange), and DiD (blue). Scale bar
11
12 is 100 μm .
13
14
15
16
17
18
19
20
21
22
23
24
25
26
27
28
29
30
31
32
33
34
35
36
37
38
39
40
41
42
43
44
45
46
47
48
49
50
51
52
53
54
55
56
57
58
59
60
61
62
63
64
65

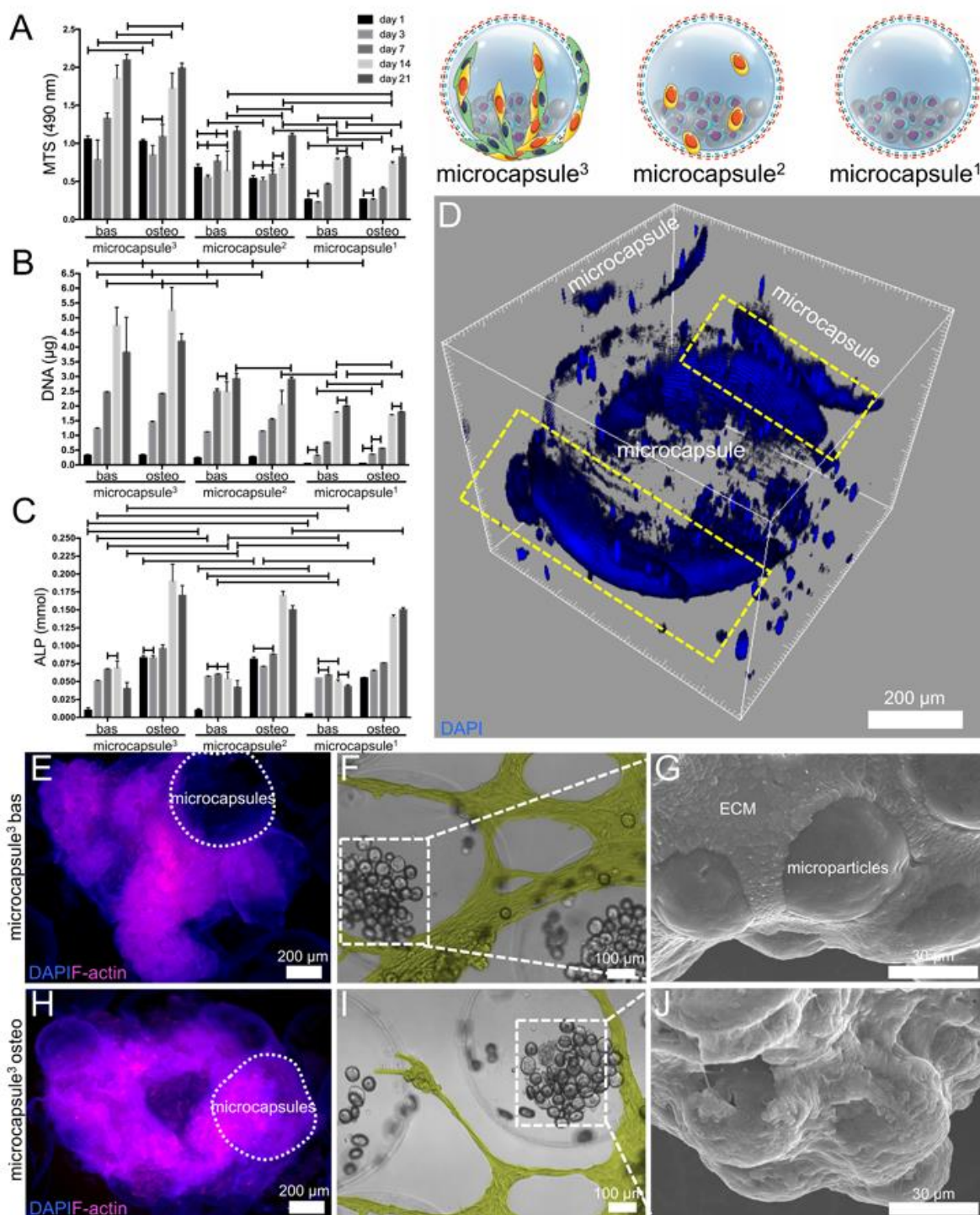


Figure 4 – (A) Metabolic activity measured at 490 nm by MTS colorimetric assay read, (B) cell proliferation evaluation by DNA quantification (µg), and (C) alkaline phosphatase (ALP) activity quantification (mmol) of microcapsules encapsulating MC3T3-E1 cells and polycaprolactone (PCL) microparticles and in contact with (i) a co-culture of fibroblasts and HUVECs (microcapsule³), (ii) a mono-culture of HUVECs (microcapsule²), or (iii) alone

(microcapsule¹). Results are presented as mean±standard deviation. Only statistically non-significant differences are marked, otherwise results are significantly different. **(D)** Overview of a liquefied microcapsule encapsulating MC3T3-E1 cells and PCL microparticles. After 8h of incubation, microcapsules were visualized by laser scanning confocal microscopy (LSCM). Cell nuclei was stained with DAPI (blue). The migration ability of cells from the 2D environment to the 3D structure provided by the RGD-membrane of microcapsules is highlighted by the yellow squares. Scale bar is 200 µm. **(E and H)** Macroaggregates of microcapsules assembled by fibroblasts and HUVECs after 7 days of culture in **(E)** basal (bas) or **(H)** osteogenic differentiation (osteo) media. Samples were visualized by fluorescence microscopy. F-actin filaments were stained by phalloidin (pink). Cell nuclei was stained with DAPI (blue). Scale bars are 200 µm. **(F and I)** Interaction of the network created by fibroblasts and HUVECs and its interaction with the microcapsules after 3 days of culture in **(F)** bas or **(I)** osteo media. Samples were visualized by light microscopy. Scale bars are 100 µm. **(G and J)** SEM images of the microaggregates composed by encapsulated MC3T3-E1 cells and PCL microparticles formed inside the liquefied core of microcapsules after 7 days of culture in **(G)** bas or **(J)** osteo media. Scale bars are 30 µm.

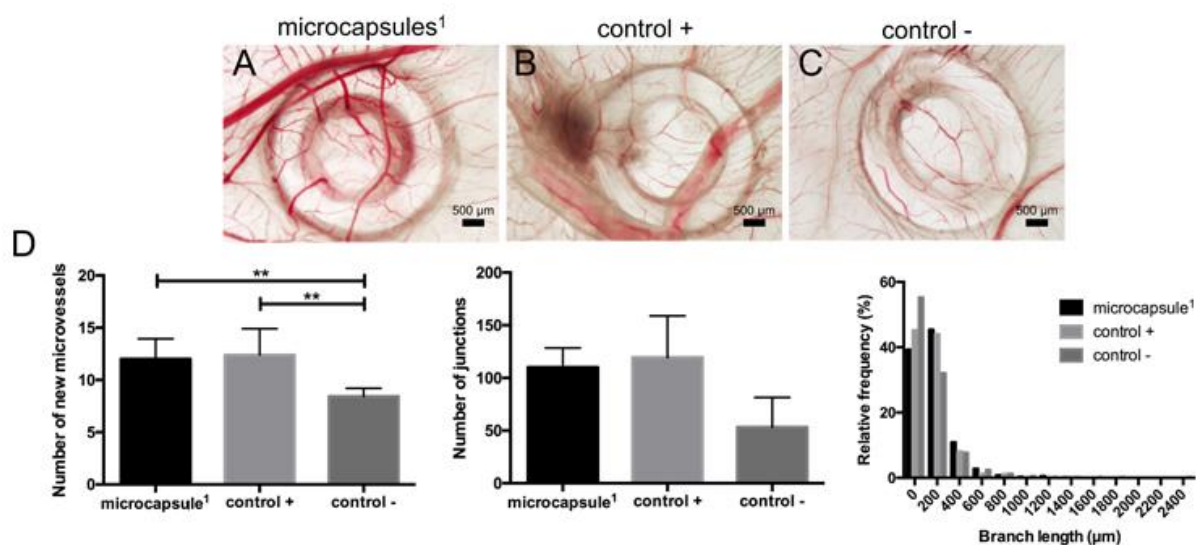


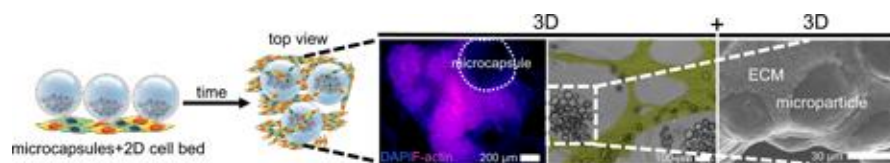
Figure 5 – Pro-angiogenic ability of microcapsules using the chick chorioallontoic membrane (CAM) assay. Optical microscopy of CAMs inoculated with (A) microcapsule¹, (B) basic fibroblast growth factor-2 (bFG-2, control +), and (C) α -MEM/1% penicillin/streptavidin (control -). Quantification normalized per area of a well-defined Region of Interest of the (C) number of new recruited microvessels (<20 μ m), number of junctions, and branch length (% relative frequency). Scale bars are 50 μ m (**p<0.01).

Liquefied microcapsules are produced at high rates by electrohydrodynamic atomization. Microcapsules present a multilayered membrane enriched with RGD domains to allow their cell-mediated aggregation. Simultaneously, cell-mediated aggregations occur at the liquefied core of microcapsules encapsulating cells and microparticles. The bottom-up concept is here term as 3D+3D. The system also present angiogenic ability, as successfully demonstrated using a CAM model.

Liquefied systems

C.R. Correia*, I.M. Bjørge, J. Zeng, M. Matsusaki, J.F. Mano*

Liquefied microcapsules as dual-microcarriers for 3D+3D bottom-up tissue engineering



Supporting Information

Liquefied microcapsules as dual-microcarriers for 3D+3D bottom-up tissue engineering

Clara R. Correia*, Isabel M. Bjørge, Jinfeng Zeng, Michiya Matsusaki, João F. Mano*

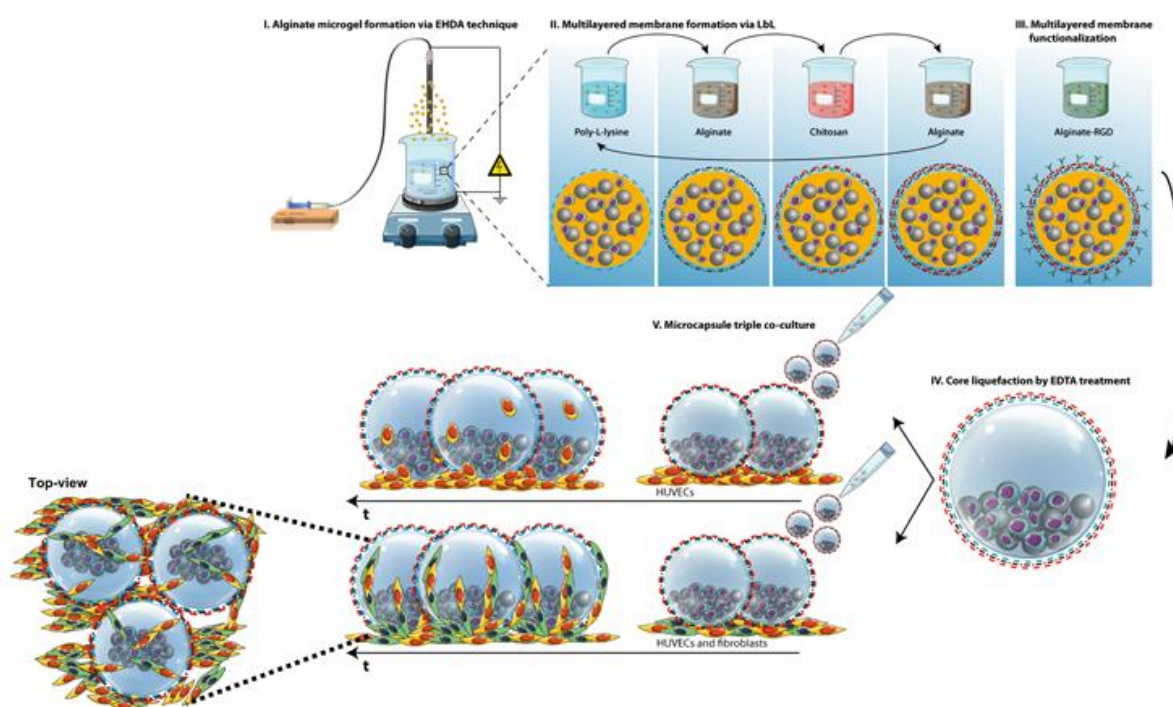
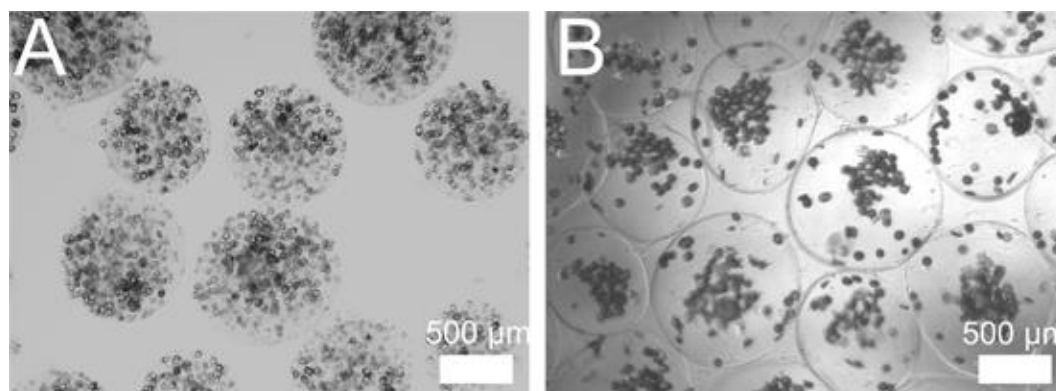
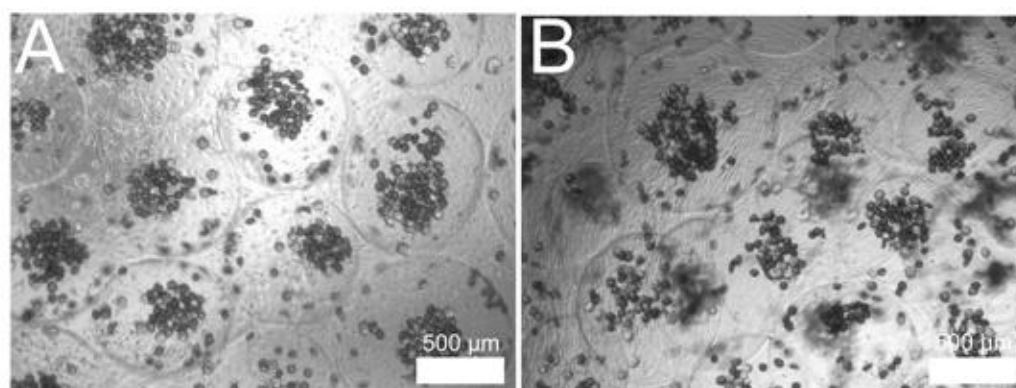


Figure S1 – Schematic representation of the production of liquefied and multilayered microcapsules, and the experimental design of the study. **(I)** Alginate microgels loaded with cells and microparticles are obtained by electrohydrodynamic atomization (EHDA) technique. Different parameters of the process are optimized, namely the alginate concentration, the flow rate, the distance between the tip to the collector, and the applied voltage. **(II)** Microgels are used as templates to produce a multilayered membrane through the assembly of three polyelectrolytes, poly(L-lysine), alginate, and chitosan, by the layer-by-layer (LbL) technique. **(III)** The last layer of microgels is functionalized by combining alginate with the cell-adhesive motif arginyl-glycyl-aspartic acid (RGD). **(IV)** Coated microcapsules are immersed in

1 ethylenediaminetetraacetic acid (EDTA) to liquefy the alginate core. (V) The obtained liquefied
2 and multilayered microcapsules are transferred to the top of previously formed 2D cell beds
3 composed by HUVECs alone or co-cultured with fibroblasts. With time, 2D cell beds start to
4 migrate towards the multilayer of microcapsules, leading to the formation of macroaggregates.
5 Simultaneously, the encapsulated cells and microparticles interact inside the liquefied core, and
6 create microaggregates. The concept is herein termed as 3D+3D bottom-up tissue engineering.
7
8
9
10
11
12
13
14
15
16



17
18
19
20
21
22
23
24
25
26
27
28
29
30
31 **Figure S2** – Microparticles and cells encapsulated in (A) alginate microgels or (B) liquefied
32 and multilayered microcapsules. Scale bars are 500 μm.
33
34
35
36



37
38
39
40
41
42
43
44
45
46
47
48
49
50
51 **Figure S3** – Liquefied and multilayered microcapsules presenting in the last layer poly(L-
52 lysine). Microcapsules are cultured on top of 2D cell beds composed by (A) HUVECs alone or
53 (B) co-cultured with fibroblasts. Scale bars are 500 μm.
54
55
56
57
58
59
60
61
62
63
64
65

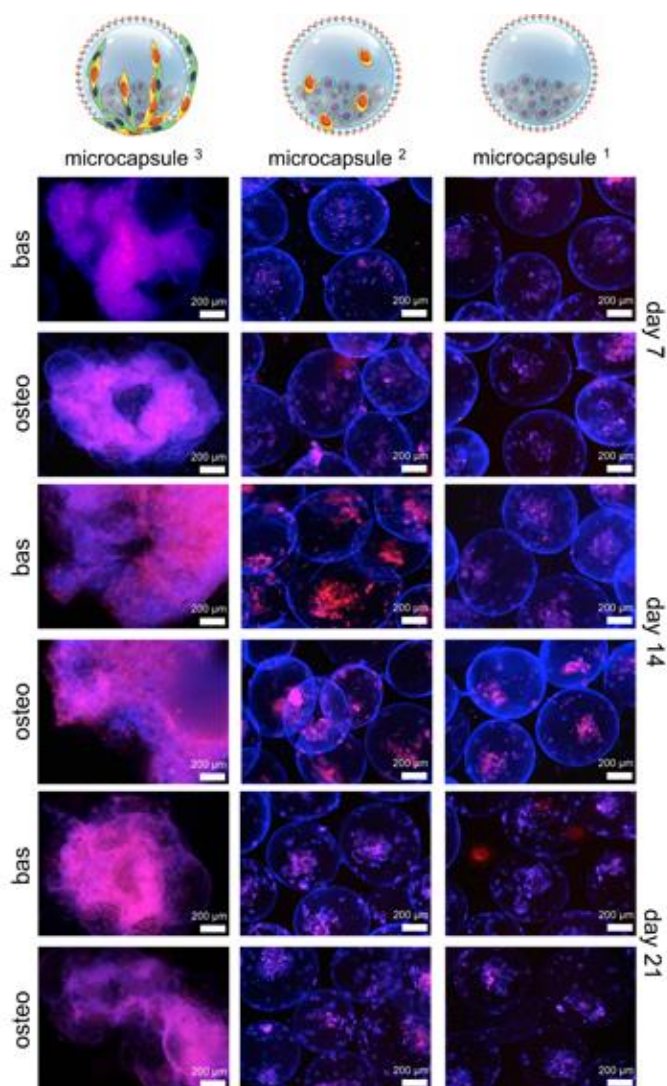


Figure S4 – Fluorescence microscopy visualization of (i) microcapsules encapsulating MC3T3-E1 cells and polycaprolactone (PCL) microparticles, and in contact with a co-culture of fibroblasts and HUVECs (microcapsule³), (ii) microcapsules encapsulating MC3T3-E1 cells and polycaprolactone (PCL) microparticles, and in contact with a mono-culture of HUVECs (microcapsule²), and (iii) microcapsules encapsulating MC3T3-E1 cells and polycaprolactone (PCL) microparticles alone (microcapsule¹). Cell nuclei was stained with DAPI (blue), and F-actin filaments with phalloidin (pink). Samples were cultured in basal (bas) or osteogenic differentiation (osteo) media and visualized at day 7, 14, and 21 post-encapsulation. Scale bars are 200 μm.

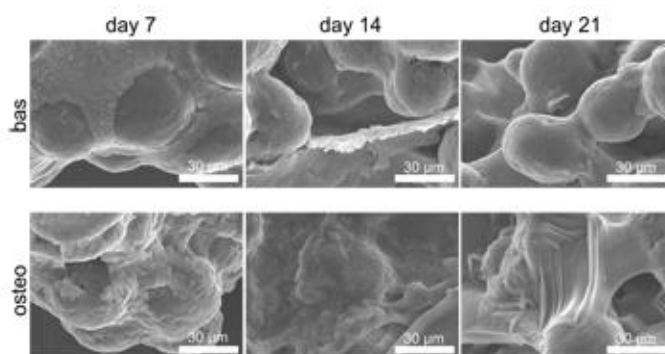


Figure S5 – SEM images of the microaggregates composed by encapsulated cells and PCL microparticles, and formed inside the liquefied environment of microcapsules³. Microcapsules were cultured in bas or osteo media and visualized at day 7, 14, and 21 post-encapsulation. Scale bars are 30 µm.



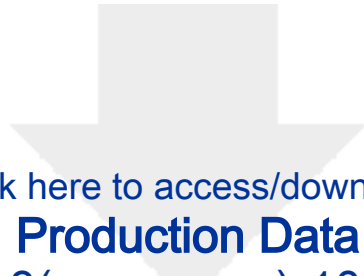
[Click here to access/download](#)

Production Data

Figure1(new-letters)-100dpi.tif







Click here to access/download
Production Data
Figure3(new-arrow)-100dpi.tif





Click here to access/download
Production Data
Figure4(new)-100.tif

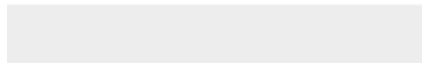
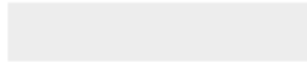




[Click here to access/download](#)

Production Data

[FigureS1\(new-topview\)-100dpi.tif](#)





Click here to access/download
Production Data
FigureS2(new)-100.tif

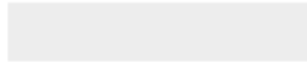




[Click here to access/download](#)

Production Data

FigureS4(100dpi).tif







Click here to access/download
Production Data
ToC(600dpi).tif